Besides the retardation, the only other approximation in this work is the neglect of the interior basis state with a radial quantum number $n\neq 0$. We showed, however, in Sec. II that these neglected states couple about 20 times more weakly to the first-order transition than the weakest-coupling channels that were taken into account.

Another open question is, of course, whether our nuclear model, which is, of course, very schematic, gives an appropriate representation of the possible virtual states. We take only a few discrete states of the whole spectrum of electron-nucleus scattering into account, namely, those such that the energy loss of the electron is $E\leq 20$ MeV. This is justified as long as one is interested in order-of-magnitude results and deals with moderate incident electron energies. If, however, the incident energy of the electron becomes large, then virtual excitations into the quasi-elastic peak, or even virtual meson production, could play a role in the dispersion effect, inasmuch as we found that the dispersion effect depends on the energy loss of the electron in a virtual excitation only through the interaction matrix elements (Sec. III). Moreover, these states form a continuum (as does the giant resonance in a more realistic model). The nuclear continuum problems which arise in electron scattering have recently been treated by applying the EKT to a nuclear shell-model Hamiltonian, while the electron was treated in Born approximation.[46] To include higher-order effects one has to apply the EKT to both the electron and the escape nucleon. Such a two-particle EKT has also been formulated.[47]

An actual calculation of this type will, however, be very involved. It therefore seems advantageous to consider the closed forms (42) (in which no explicit reference is made to the intermediate states) or (41) (which can be evaluated by the use of sum rules) for further applications of the eigenchannel theory to electron scattering.

ACKNOWLEDGMENTS

Our calculations are based on DWBA program which was lent us by Dr. D. Drechsel. We thank him and Dr. W. Scheid for many discussions and for helpful advice. The numerical work was done with the Burroughs 5500 at the Computer Science Center of the University of Virginia. We acknowledge the kind cooperation of its staff. Furthermore, we gratefully acknowledge the kind hospitality of Professor W. D. Whitehead at the Center for Advanced Studies of the University of Virginia.

[46] P. Antony-Spies, W. Donner, H. G. Wahsweiler, and W. Greiner, Phys. Letters **26B**, 268 (1968).

[47] M. Danos and W. Greiner, Z. Physik **202**, 125 (1967); H. J. Weber and W. Greiner, University of Virginia Report, 1968 (unpublished).

PHYSICAL REVIEW VOLUME 186, NUMBER 4 20 OCTOBER 1969

Measurement of Polarization Effects in the $H^2(d, p)H^3$ Reaction at 140 keV*†

R. I. STEINBERG, C. W. DRAKE,‡ AND D. C. BONAR
Gibbs Laboratory, Yale University, New Haven, Connecticut 06520
(Received 26 May 1969)

The vector analyzing power $D_2(\theta)$ and the tensor analyzing powers $D_{33}(\theta)$ and $[D_{11}(\theta)-D_{22}(\theta)]$ of the $H^2(d, p)H^3$ reaction have been measured at a mean deuteron energy of 140 keV using a beam of polarized deuterons from the Yale polarized-ion source and a 100-keV-thick target of unpolarized deuterated polyethylene. The results for the vector analyzing power are in agreement with previous measurements by Ad'yasevich *et al.* at 100 and 200 keV and are consistent with a theoretical treatment by Rook and Goldfarb. In the notation of this treatment, the results are $B_3/B_0=0.321\pm0.059$ and $B_4/B_0=-0.036\pm0.042$. The results for the tensor analyzing powers are in reasonable agreement with a previous measurement by Ad'yasevich *et al.* at 165 keV and are not consistent with the Rook-Goldfarb treatment in that a small contribution from quintet-state reaction matrix elements is apparent. The experimental results for the tensor analyzing powers are given by $B_5/B_0=-0.059\pm0.015$, $B_5'/B_0=-0.556\pm0.102$, and $B_7/B_0=-0.413\pm0.152$. The quintet-state contributions, in the notation introduced in this paper, are measured to be $B_8/B_0=-0.148\pm0.084$ and $B_{11}/B_0=0.002\pm0.009$. A calculation is made in which the assumptions of the Rook-Goldfarb treatment are relaxed in order to allow nonvanishing s-wave quintet-state reaction matrix elements. Explicit expressions for the various contributions of these reaction matrix elements to the differential cross section are presented.

I. INTRODUCTION

SINCE its discovery by Lawrence, Livingston, and Lewis[1] in 1933, the $H^2(d, p)H^3$ reaction has been the subject of a great number of investigations, both theoretical and experimental. The main point of interest for the earliest work was the 1936 discovery[2] that the angular distribution of the outgoing protons was anisotropic in the c.m. system even at energies as low as 100 keV. This fact indicated that p-wave contributions to the reaction were important at these low energies.

* Research supported by the U.S. Atomic Energy Commission.
† Based on a dissertation submitted by R.I.S. to the faculty of Yale University in candidacy for the Ph.D. degree.
‡ Present address: Oregon State University, Corvallis, Ore. 97331.

[1] E. O. Lawrence, M. S. Livingston, and G. N. Lewis, Phys. Rev. **44**, 56(L) (1933).

[2] A. E. Kempton, B. C. Browne, and R. Maasdorp, Proc. Roy. Soc. (London) **A157**, 386 (1936).

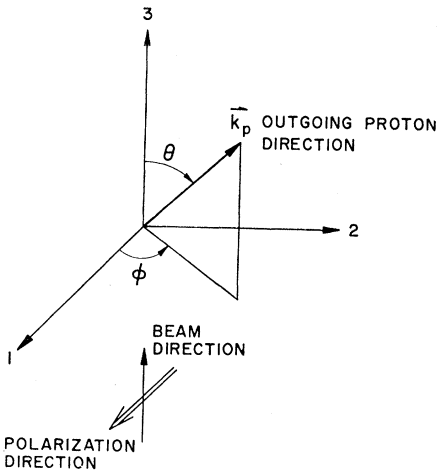

FIG. 1. Coordinate system used for the description of the $H^2(d, p)H^3$ reaction with incident deuterons polarized transverse to the direction of beam propagation. The polarization direction is indicated by the double-shafted arrow.

In 1948, following extensive measurements of the energy dependence of the anisotropy,[3] Konopinski and Teller pointed out[4] that noncentral forces were required in order to explain the experimental results. Because the existence of these forces suggested that the reaction would be sensitive to the polarization state of the incident deuteron beam and because of the current availability of sources of polarized deuterons, interest has recently been growing in the study of polarization effects in this reaction. Presently available experimental results on the $H^2(d, p)H^3$ reaction with polarized incident deuterons are given in Refs. 5–11. The present work utilizes a polarized-ion source which is quite different from those of Refs. 5–11. The Yale polarized-ion source consists of an atomic-beam magnetic-resonance device utilizing the classic Rabi two-wire magnetic field geometry. Although its beam intensity is low ($\approx\frac{1}{2}$ nA) by current standards, this source has the advantage of allowing the beam polarization to be changed merely by switching an rf frequency. Because of this feature, many possible sources of systematic error are eliminated. For example, it is unnecessary to change any magnetic fields in order to reverse the sign of the vector polarization.

The results of these measurements have been reported in preliminary form in Refs. 12 and 13.

II. THEORY OF THE $H^2(d, p)H^3$ REACTION

A. Relationship between Analyzing Powers and Differential Cross Section

The differential cross section $\sigma_p(\theta, \varphi)$ for a reaction with polarized incident spin-1 particles and unpolarized target has been given in terms of the unpolarized cross section $\sigma_0(\theta)$ by[14]

$$\sigma_p(\theta, \varphi) = \sigma_0(\theta)[1+\tfrac{3}{2}\mathbf{P}\cdot\mathbf{P}^A+\tfrac{1}{2}P_{33}P_{33}^A +\tfrac{2}{3}(P_{12}P_{12}^A+P_{13}P_{13}^A+P_{23}P_{23}^A) +\tfrac{1}{6}(P_{11}-P_{22})(P_{11}^A-P_{22}^A)], \quad (1)$$

where the coordinate system is shown in Fig. 1, where the quantities $\mathbf{P}$ and P_{ij}, the polarization vector and tensor, respectively, define the polarization state of the incident beam, and where the functions $\mathbf{P}^A$ and P_{ij}^A are characteristic of the reaction and completely describe the effect of beam polarization on the differential cross section. These functions are therefore known as the vector and tensor analyzing powers, respectively.

In the present experiment, the only nonvanishing components of the polarization vector and tensor were given by

$$P_{11}=P_{33}^*, \qquad P_{22}=P_{33}=-\tfrac{1}{2}P_{33}^*, \quad (2)$$

and

$$P_1=P_3^*$$

(where the notation P_{33}^* for the tensor polarization and P_3^* for the vector polarization arises from the fact that these quantities are described in the atomic-beam system, in which the polarization axis is taken as the three-axis; whereas the coordinate system for describing the nuclear reaction uses the beam propagation direction for the three-axis). Values of P_3^* and P_{33}^* are given in Fig. 2 for each of the available rf transitions. Since P_{12}, P_{13}, and P_{23} were zero in this experiment, only two of the tensor analyzing powers were determined: P_{33}^A and $(P_{11}^A-P_{22}^A)$.

Under the assumption of parity conservation, the

[3] H. P. Manning, R. D. Huntoon, F. Myers, and V. Young, Phys. Rev. **61**, 371 (1942); R. D. Huntoon, A. Ellett, D. S. Bayley, and J. A. Van Allen, *ibid.* **58**, 97 (1940); E. Bretscher, A. French, and F. Seidl, *ibid.* **73**, 815 (1948).

[4] E. J. Konopinski and E. Teller, Phys. Rev. **73**, 822 (1948).

[5] D. Fick, R. Fleischmann, and G. Graw, in *Proceedings of the Second International Symposium on Polarization Phenomena of Nucleons, Karlsruhe, 1965*, edited by P. Huber and H. Schopper (W. Rusch and Co., Bern, 1966), p. 359.

[6] H. A. Christ and L. Brown, Nucl. Phys. **79**, 473 (1966).

[7] C. Petitjean, P. Huber, H. Paetz gen. Schieck, and H. R. Striebel, Helv. Phys. Acta **40**, 401 (1967).

[8] B. P. Ad'yasevich, Yu. P. Polunin, and D. E. Fomenko, Yadern. Fiz. **5**, 713 (1967) [English transl.: Soviet J. Nucl. Phys. **5**, 507 (1967)].

[9] B. P. Ad'yasevich, V. G. Antonenko, P. A. Kuznetsov, Yu. P. Polunin, and D. E. Fomenko, Yadern. Fiz. **8**, 267 (1968) [English transl.: Soviet J. Nucl. Phys. **8**, 154 (1968)].

[10] F. A. Gückel, H. W. Franz, and D. Fick, Z. Physik **214**, 321 (1968).

[11] D. Fick and H. W. Franz, Phys. Letters **27B**, 541 (1968); H. W. Franz and D. Fick, Nucl. Phys. **A122**, 591 (1968).

[12] D. C. Bonar, R. I. Steinberg, and C. W. Drake, Bull. Am. Phys. Soc. **13**, 98 (1968).

[13] R. I. Steinberg, D. C. Bonar, and C. W. Drake, Bull. Am. Phys. Soc. **14**, 22 (1969).

[14] L. J. B. Goldfarb, Nucl. Phys. **7**, 622 (1958).

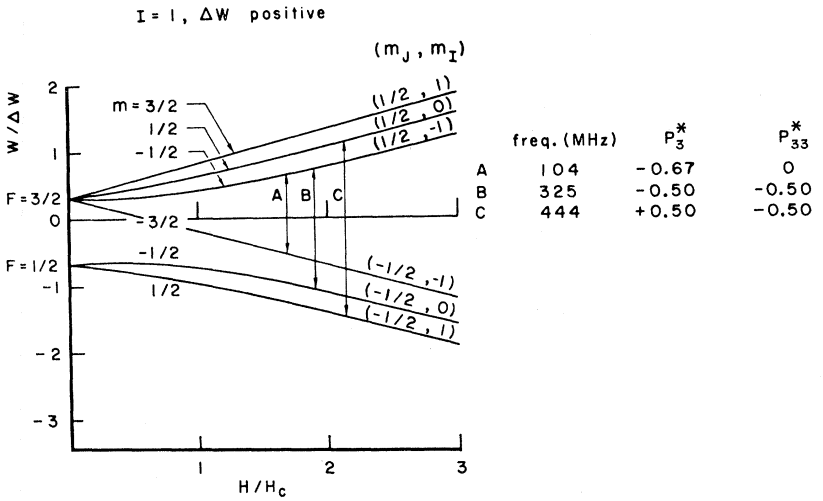

FIG. 2. Energy-level diagram for deuterium in a magnetic field H/H_c, where $H_c \approx 117$ G. ΔW is the hyperfine-structure separation of deuterium, 327.38 MHz. Available rf transitions are indicated, together with their frequencies and the theoretical polarizations obtained. The latter are calculated for equal ionization of the two refocused states in a 4-G field. The transitions, which were induced at 75 G, are shown at different values of H/H_c only for purposes of clarity.

following relationships are obtained[15]:

$$P_1^A(\theta,\varphi) = D_1(\theta)\ \sin\varphi,$$
$$P_2^A(\theta,\varphi) = D_2(\theta)\ \cos\varphi,$$
$$P_3^A(\theta,\varphi) = 0,$$
$$P_{33}^A(\theta,\varphi) = D_{33}(\theta),$$
$$P_{11}^A(\theta,\varphi) - P_{22}^A(\theta,\varphi) = [D_{11}(\theta) - D_{22}(\theta)]\ \cos 2\varphi, \quad (3)$$
$$P_{12}^A(\theta,\varphi) = D_{12}(\theta)\ \sin 2\varphi,$$
$$P_{13}^A(\theta,\varphi) = D_{13}(\theta)\ \cos\varphi,$$

and

$$P_{23}^A(\theta,\varphi) = D_{23}(\theta)\ \sin\varphi,$$

where the D functions satisfy the relations

$$D_1(\theta) = -D_2(\theta),$$
$$D_{23}(\theta) = D_{13}(\theta), \quad (4)$$

and

$$D_{12}(\theta) = D_{11}(\theta) - D_{22}(\theta).$$

In view of Eqs. (4), it is seen that only four of the D functions in Eqs. (3) are independent: $D_2(\theta)$, $D_{33}(\theta)$, $D_{13}(\theta)$, and $D_{11}(\theta) - D_{22}(\theta)$. In any reaction, furthermore, the maximum and minimum values allowed for these analyzing powers are

$$D_2(\theta)_{\max} = +1,$$
$$D_2(\theta)_{\min} = -1,$$
$$D_{33}(\theta)_{\max} = +1,$$
$$D_{33}(\theta)_{\min} = -2,$$
$$D_{13}(\theta)_{\max} = +\tfrac{3}{2},$$
$$D_{13}(\theta)_{\min} = -\tfrac{3}{2},$$

and

$$[D_{11}(\theta) - D_{22}(\theta)]_{\max} = +3,$$
$$[D_{11}(\theta) - D_{22}(\theta)]_{\min} = -3.$$

[15] H. Bürgisser, E. Baumgartner, R. E. Benenson, G. Michel, F. Seiler, and H. R. Striebel, Helv. Phys. Acta **40**, 185 (1967).

In the alternative spherical tensor-moment representation, the four independent analyzing powers are denoted by iT_{11}', T_{20}', T_{21}', and T_{22}', where the relations between the two sets of analyzing powers are

$$D_2(\theta) = (-2/\sqrt{3})\, iT_{11}'(\theta),$$
$$D_{33}(\theta) = \sqrt{2}T_{20}'(\theta),$$
$$D_{13}(\theta) = -\sqrt{3}T_{21}'(\theta),$$

and

$$D_{11}(\theta) - D_{22}(\theta) = 2\sqrt{3}T_{22}'(\theta).$$

Substitution of Eqs. (2)–(4) into Eq. (1) leads to

$$\sigma_p(\theta,\varphi) = \sigma_0(\theta)\{1 - \tfrac{3}{2}P_3^* D_2(\theta)\ \sin\varphi - \tfrac{1}{4}P_{33}^* D_{33}(\theta) + \tfrac{1}{4}P_{33}^*[D_{11}(\theta) - D_{22}(\theta)]\ \cos 2\varphi\}, \quad (5)$$

which is the desired relationship between the analyzing powers and the differential cross section for the present experiment.

B. Calculation of Analyzing Powers

The analyzing powers of the $H^2(d,p)H^3$ reaction have been calculated by Rook and Goldfarb[16] subject to

TABLE I. Initial- and final-state quantum numbers for the reaction matrix elements included in the calculation of the $H^2(d,p)H^3$ analyzing powers. The initial-state quantum numbers are denoted by $S'l'J$, the final-state quantum numbers by SlJ. The notation for the matrix elements follows that of Ref. 16.

Matrix elements	S'	l'	J	S	l
α_0	0	0	0	0	0
α_{10}	1	1	0	1	1
α_{11}	1	1	1	1	1
α_{12}	1	1	2	1	1
β_{11}	1	1	1	0	1
α_2	0	2	2	0	2
β_2	0	2	2	1	2
γ_{02}	2	0	2	0	2
δ_{02}	2	0	2	1	2

[16] J. R. Rook and L. J. B. Goldfarb, Nucl. Phys. **27**, 79 (1961).

the following assumptions: In the entrance channel, partial waves beyond d waves may be neglected and d waves need to be considered only in interference with s waves; in the exit channel, all partial waves higher than d waves can be excluded; and quintet-state collisions of the two-deuteron system may be ignored.

In order to investigate the validity of this last assumption, the calculation has been extended to include the possibility of quintet-state effects. The assumptions of this calculation were identical with those of the previous one[16] except for the inclusion of s-wave quintet reaction matrix elements, of which only two exist. Other possible quintet matrix elements are d-wave and higher and were not included in the calculation. Since the quintet elements were expected to be relatively small, terms involving the product of two of them were neglected.

The nine reaction matrix elements included in the calculation are listed in Table I together with the initial- and final-state quantum numbers for each element. The two s-wave quintet-state matrix elements are denoted by γ_{02} and δ_{02}, where the γ-matrix elements describe quintet-singlet transitions and the δ elements describe quintet-triplet transitions.

The procedure used was the tensor moment method.[17] A version of program TENMO,[18] modified to allow for the identity of the initial particles, was used. The results of the calculation are given by

$$D_2(\theta)=\tfrac{2}{3}[W_0(\theta)]^{-1}\times\left(\frac{B_3}{B_0}P_{11}(\cos\theta)+\frac{B_4}{B_0}P_{21}(\cos\theta)\right),$$

$$D_{33}(\theta)=\frac{2}{W_0(\theta)}\left(\frac{B_7}{B_0}+\frac{B_8}{B_0}P_1(\cos\theta)+\frac{B_5'}{B_0}P_2(\cos\theta)+\frac{B_9}{B_0}P_3(\cos\theta)+\frac{B_{10}}{B_0}P_4(\cos\theta)\right), \quad (6)$$

$$D_{11}(\theta)-D_{22}(\theta)=\frac{3}{W_0(\theta)}\left(\frac{B_5}{B_0}P_{22}(\cos\theta)+\frac{B_{11}}{B_0}P_{32}(\cos\theta)+\frac{B_{12}}{B_0}P_{42}(\cos\theta)\right),$$

and

$$D_{13}(\theta)=\tfrac{3}{2}[W_0(\theta)]^{-1}\times\left(\frac{B_{13}}{B_0}P_{11}(\cos\theta)+\frac{B_6}{B_0}P_{21}(\cos\theta)+\frac{B_{14}}{B_0}P_{31}(\cos\theta)+\frac{B_{15}}{B_0}P_{41}(\cos\theta)\right),$$

where $W_0(\theta)$ is the unpolarized angular distribution [see Eq. (11)], P_{lm} is an associated Legendre function, and where

$$B_0=|\alpha_0|^2+|\alpha_{10}|^2+3|\alpha_{11}|^2+3|\beta_{11}|^2+5|\alpha_{12}|^2,$$

$$B_3=\mathrm{Im}(5.196\alpha_0\beta_{11}^*-4.108\gamma_{02}\beta_{11}^*-3.558\delta_{02}\alpha_{11}^*+3.558\delta_{02}\alpha_{12}^*),$$

$$B_4=\mathrm{Im}(\tfrac{3}{2}\alpha_{10}\alpha_{12}^*+\tfrac{9}{4}\alpha_{11}\alpha_{12}^*),$$

$$B_5=\tfrac{3}{8}|\alpha_{12}|^2+\tfrac{3}{8}|\alpha_{11}|^2-\tfrac{3}{4}|\beta_{11}|^2+\mathrm{Re}(-\tfrac{3}{4}\alpha_{12}\alpha_{11}^*+1.054\gamma_{02}\alpha_0^*-1.506\gamma_{02}\alpha_2^*-0.753\delta_{02}\beta_2^*),$$

$$B_6=\tfrac{1}{2}|\alpha_{12}|^2+\mathrm{Re}(\alpha_{12}\alpha_{10}^*-\tfrac{3}{2}\alpha_{12}\alpha_{11}^*+2.108\gamma_{02}\alpha_0^*+1.506\gamma_{02}\alpha_2^*+0.753\delta_{02}\beta_2^*),$$

$$B_5'=2B_6-B_5,$$

$$B_7=\tfrac{1}{4}(|\alpha_{12}|^2-3|\beta_{11}|^2-3|\alpha_{11}|^2+2|\alpha_{10}|^2)+3.162\,\mathrm{Re}(\gamma_{02}\alpha_2^*+\delta_{02}\beta_2^*), \quad (7)$$

$$B_8=\mathrm{Re}(-4.930\gamma_{02}\beta_{11}^*-4.269\delta_{02}\alpha_{11}^*-1.423\delta_{02}\alpha_{12}^*),$$

$$B_9=\mathrm{Re}(4.930\gamma_{02}\beta_{11}^*-2.846\delta_{02}\alpha_{11}^*-5.692\delta_{02}\alpha_{12}^*),$$

$$B_{10}=\mathrm{Re}(8.132\gamma_{02}\alpha_2^*-5.421\delta_{02}\beta_2^*),$$

$$B_{11}=\tfrac{1}{9}B_9,$$

$$B_{12}=\tfrac{1}{18}B_{10},$$

$$B_{13}=B_8,$$

$$B_{14}=\tfrac{4}{9}B_9,$$

$$B_{15}=\tfrac{1}{3}B_{10}.$$

It is seen that, subject to the above assumptions, only the nonvanishing of quintet-state matrix elements can yield finite values for the coefficients B_8–B_{15}. Furthermore, the coefficients B_8, B_9, B_{11}, B_{13}, and B_{14} lead to the appearance in the tensor analyzing powers of Legendre functions of odd order. The presence of a contribution from odd-order Legendre functions in these analyzing powers is readily detectable experimentally by noting the symmetry properties of the measured curves with respect to the substitution $(\pi-\theta)$ for θ. For odd values of m, odd-order Legendre functions are symmetric with respect to this substitution, while for even values of m, these functions are antisymmetric. As may be shown from Eq. (146) of Ref. 17, moreover, no combination of singlet and triplet matrix elements can lead to Legendre functions of odd order, regardless of how high a partial wave to which the matrix elements belong. (For an explicit proof of this statement, see Ref. 19.) Detection of odd-order Legendre functions in the tensor analyzing powers thus constitutes unambiguous proof of quintet-state collisions.[20]

[17] T. A. Welton, *Fast Neutron Physics*, edited by J. B. Marion and J. L. Fowler (Wiley-Interscience, Inc., New York, 1963), Vol. II, p. 1317.

[18] R. D. McCulloch, H. W. Graben, S. T. Thornton, and H. B. Willard, Oak Ridge National Laboratory Report No. ORNL-4125, 1967 (unpublished).

[19] R. I. Steinberg, Ph.D. thesis, Yale University, 1969, p. 105 (unpublished).

[20] The participation of quintet-state collisions in the reaction was first pointed out by Goldfarb in a private communication noted in Ref. 7. See also L. J. B. Goldfarb and H. E. Reed, Phys. Letters **27B**, 140 (1968).

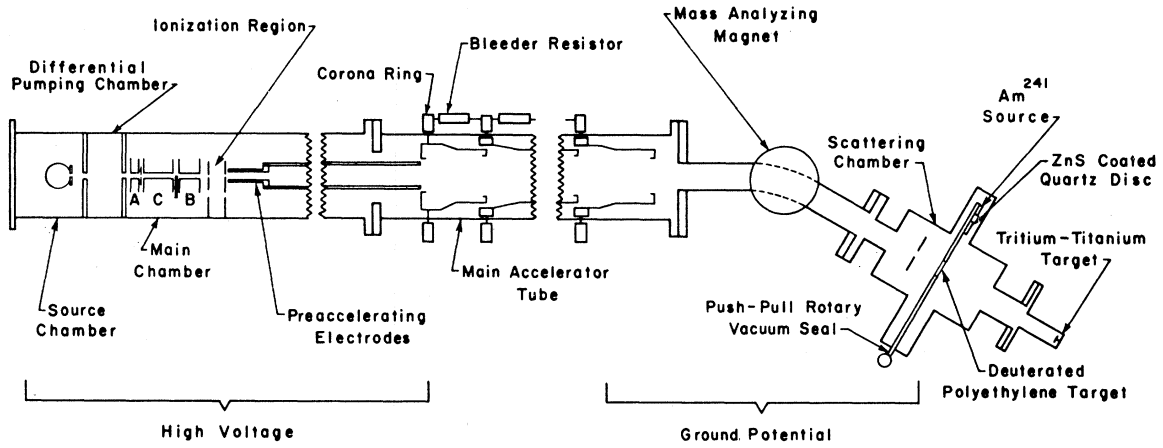

FIG. 3. Over-all schematic diagram of the experiment, showing atomic-beam magnetic-resonance spectrometer mounted at high potential, together with electrostatic accelerator and scattering chamber where the $H^2(d,p)H^3$ and $H^3(d,n)He^4$ reactions were induced.

III. APPARATUS

A. Description

A schematic diagram of the experimental arrangement is shown in Fig. 3. For the present experiment the polarized-ion source has been mounted on a high-voltage platform, as indicated in Fig. 3. The atomic-beam magnetic-resonance apparatus used for the production of polarized deuterium atoms has been described previously.[21,22] After passing through the detector slit of the atomic-beam apparatus, the polarized atoms were ionized by an electron-bombardment ionizer, which is described below. After extraction from the ionization region, the ions were focused and accelerated to about 15 keV by means of the preaccelerating electrodes. The beam then entered the main accelerator tube where it was electrostatically accelerated to the final energy of 190 keV. The beam was momentum analyzed by a deflecting magnet before entering the scattering chamber. Once inside this chamber, the beam struck a target of deuterated polyethylene. Outgoing protons from the $H^2(d,p)H^3$ reaction were detected by solid-state detectors. The polarization and background contamination of the beam were monitored continuously during data collection by allowing a small fraction of the beam to pass through an aperture in the polyethylene target and continue on to a thick tritiated-titanium target where the $H^3(d,n)He^4$ reaction took place. The 14-MeV neutrons produced by this reaction were detected by plastic scintillation detectors mounted outside the vacuum system. This method largely eliminated systematic errors caused by fluctuation of the polarization and background contamination.

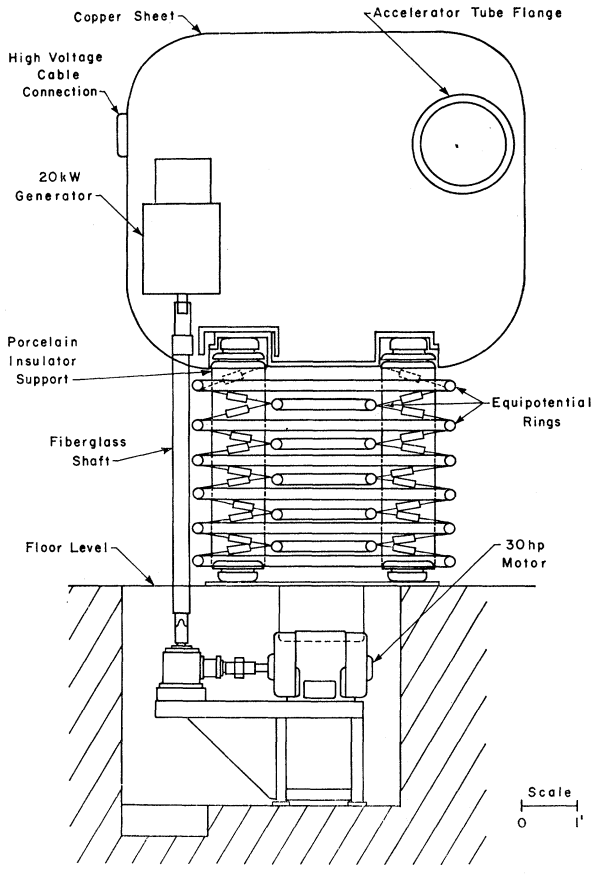

FIG. 4. Diagram of the high-voltage platform on which was mounted the entire polarized-ion source.

B. Design

The most important modifications of the apparatus described in Refs. 21 and 22 are mounting of the polarized-ion source on a high-voltage platform, design and construction of a new electron-bombardment

[21] V. W. Hughes, C. W. Drake, D. C. Bonar, J. S. Greenberg, and G. F. Pieper, Helv. Phys. Acta. Suppl. 6, 89 (1960); *ibid.* 6, 435 (1960).

[22] D. C. Bonar, C. W. Drake, R. D. Headrick, and V. W. Hughes, Phys. Rev. 174, 1200 (1968).

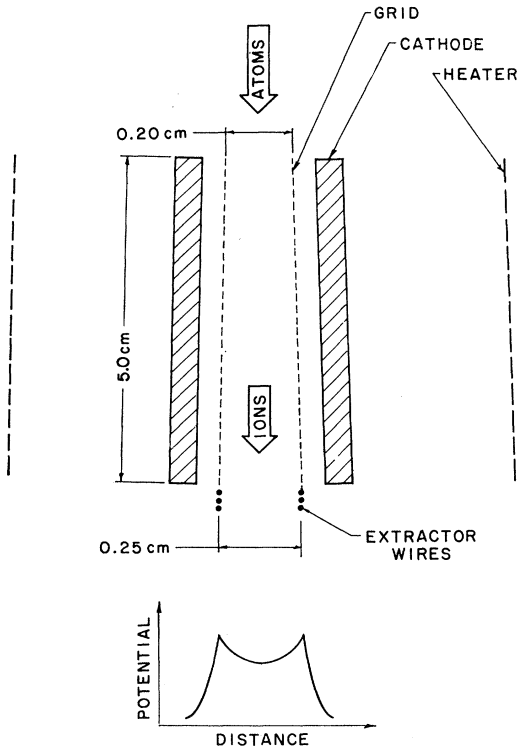

FIG. 5. Schematic diagram of the electron-bombardment ionizer. Also shown is a plot of electrostatic potential versus distance for a typical transverse section of the gun.

ionizer, mass analysis of the beam, and construction of a suitable scattering chamber. These modifications will be discussed below.

1. High-Voltage Platform

The polarized-ion source was mounted on the high-voltage platform shown in Fig. 4. The enclosure was designed for voltages up to 600 kV; however, at the voltage of 190 kV used for the present measurements, it was not found necessary to enclose the ion source completely. ac power for the source was derived from a generator driven by an electric motor through a rotating nonconducting shaft. High-voltage dc power was supplied to the platform from a 600-kV insulating-core transformer. Chilled deionized water and compressed air needed for the operation of the source were supplied through plastic pipes. Two Plexiglas light pipes were used to control the polarization mode of the source. The high voltage was measured by means of a rotating-vane generating voltmeter which was calibrated against a high-resistance voltmeter of 3% accuracy.

2. Ionizer

A schematic top view of the new ionizer is shown in the upper part of Fig. 5. Electrons emitted from two Philips cathodes, one on each side of the atomic-beam trajectory, were accelerated toward the atomic beam by two grids. After crossing the atomic beam, the electrons were collected by these grids. The space charge due to the presence of electrons between the grids produced a depression of the electrostatic potential in this region. The resulting potential distribution is diagrammed at the bottom of Fig. 5. Ions formed by collision of the electrons with the atomic beam were trapped in the potential well. In order to extract these ions, the gun was designed so that the intergrid spacing gradually increased toward the exit end. The increasing grid spacing produced a deepening of the potential well which caused extraction of the ions. The intensity of the beam of D^+ ions from the ionizer, measured after acceleration, was typically 1.3 nA with rf on and 0.8 nA with rf off. Thus, 0.5 nA of polarized D^+ ions were obtained after subtraction of the "rf-off" current from the "rf-on" current. The 0.8 nA of rf-off current resulted from ionization of background deuterium gas, and was therefore unpolarized. The over-all efficiency of the ionizer was estimated to be greater than 3×10^{-3}. The gun operated quite reliably for periods of 300–400 h. An unexpected difficulty, however, was encountered in the form of a 25–50% loss of polarization. The precise mechanism of this partial depolarization is not clearly understood but is thought to be due either to the formation of trapping regions in the space-charge-induced potential gradient as a result of nonuniformities in cathode emission or to collisional processes with background atoms in the ionization region.

3. Momentum Analysis

After electrostatic acceleration, the beam entered a 30° bending magnet for momentum analysis. The lower exit port of the magnet led directly into the

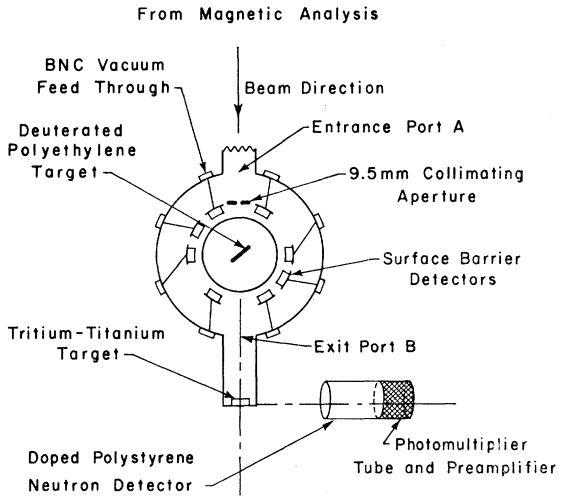

FIG. 6. Diagram of the scattering chamber where the $H^2(d, p)H^3$ and $H^3(d, n)He^4$ reactions took place. The neutron detector in the drawing was at a 0° angle with respect to the polarization axis; a second detector, not shown, was placed at 90°. These two neutron counters were used to measure the 0°/90° asymmetry of the neutron angular distribution as a check on the beam tensor polarization.

scattering chamber, while two other ports were provided with ZnS-coated windows for viewing the beam.

4. *Scattering Chamber*

A schematic top view of the scattering chamber is shown in Fig. 6. The momentum-analyzed beam was collimated by a circular aperture before striking the target. The 100-keV-thick deuterated-polyethylene target was mounted on a 1-mg/cm^2 backing of Al foil. Although thick enough to completely stop the incident deuteron beam, the backing permitted outgoing 3.5 MeV protons to escape with only a 70-keV energy loss. Multiple Coulomb scattering of the outgoing protons was calculated to be less than 1 deg and was therefore not a serious problem. A 1-mm-diam hole in the Al backing allowed a fraction of the beam to reach a thick target of tritiated titanium. Surrounding the deuterated-polyethylene target was an array of eight Si surface-barrier detectors. The detectors were placed at a distance of 37 mm from the target, subtending a half-angle of approximately 8°.

To study the azimuthal dependence of the angular distribution, the entire scattering chamber could be rotated about the beam axis.

IV. METHODS

The transitions used for the present experiment are indicated by B and C on the Breit-Rabi diagram shown in Fig. 2. The theoretical vector and tensor polarizations obtained from these transitions are also shown in that illustration. Because of the partial depolarization mentioned above, it was necessary to monitor the beam polarization continuously. The tensor polarization was obtained by measurement of the 0°/90° asymmetry of the $H^3(d,n)He^4$ neutrons. The sensitivity of this reaction to tensor polarization had been experimentally confirmed.[23] The value of the vector polarization was then determined from knowledge of the tensor polarization. The principal assumption used in this determination was that the depolarization was attributable to partial admixture of background deuterium atoms into the polarized beam. With this assumption it is clear that the percentage depolarization of the vector polarization is the same as that of the tensor polarization.

TABLE II. Experimental values for the analyzing powers of the $H^2(d,p)H^3$ reaction at 140-keV mean deuteron energy.

c.m. angle	D_2	D_{33}	$(D_{11}-D_{22})$
33.2°	0.04±0.07	−1.21±0.23	−0.07±0.23
94.6°	0.13±0.10	−0.37±0.31	−0.80±0.31
123.3°	0.17±0.09	−0.52±0.30	−0.34±0.30
151.6°	0.17±0.09	−1.09±0.34	−0.07±0.34
152.4°	0.20±0.08	−1.06±0.25	−0.15±0.25
92.2°	0.26±0.09	−0.31±0.28	−0.58±0.28
63.5°	0.35±0.09	−0.84±0.30	−0.44±0.30
31.1°	0.03±0.07	−1.58±0.23	−0.09±0.23

[23] E. Baumgartner, L. Brown, P. Huber, H. Rudin, and H. R. Striebel, Phys. Rev. Letters **5**, 154 (1960); H. Rudin *et al.*, Helv. Phys. Acta. **34**, 58 (1961).

TABLE III. Values for the least-squares coefficients [see Eq. (10)].

a_1	0.214±0.039
a_2	−0.024±0.028
b_0	−0.826±0.303
b_1	−0.297±0.167
b_2	−1.112±0.204
c_2	−0.177±0.046
c_3	0.006±0.028

The actual data collection was performed by alternating 6-sec periods of "rf on" with equal periods of "rf off." In this way, many possible sources of systematic error were eliminated. For the determination of the tensor analyzing powers it was found possible to double the polarized-beam intensity by running transitions B and C simultaneously. Because these transitions produced equal tensor polarizations of $-\frac{1}{2}$ and opposite vector polarizations of $-\frac{1}{2}$ and $+\frac{1}{2}$, respectively, simultaneous excitation of the two transitions resulted in a beam with tensor polarization of $-\frac{1}{2}$ and zero vector polarization, assuming equal transition probabilities. All measurements of the tensor analyzing powers used this method of simultaneous transitions. Corrections were applied for the small systematic error caused by inequality of the two transition probabilities.

V. RESULTS

A. Data Analysis

The ratio of polarized to unpolarized cross sections at each angle was determined from the expression

$$\frac{\sigma_p(\theta,\varphi)}{\sigma_0(\theta)}=R\frac{N_{\rm on}-N_{\rm off}}{N_{\rm off}}, \tag{8}$$

where $N_{\rm on}$ and $N_{\rm off}$ were the numbers of proton counts recorded with "rf on" and "rf off," respectively, and where the normalizing factor R was the ratio of unpolarized- to polarized-beam intensities. R was determined by data from the $H^3(d,n)He^4$ reaction by means of the expression

$$R=\frac{M_{\rm off}-M_{\rm cr}}{M_{\rm on}-M_{\rm off}}(1-\tfrac{1}{2}P_{33}^*), \tag{9}$$

where $M_{\rm on}$ and $M_{\rm off}$ are the counts recorded by the 0° neutron counter with "rf on" and "rf off," where $M_{\rm cr}$ is the cosmic-ray background recorded by that counter, and where the factor within the parentheses is a correction for the anisotropy caused by beam tensor polarization.

Experimental values for the cross-section ratios were obtained from Eq. (8) for the half-planes characterized by $\varphi=0$, $\frac{1}{2}\pi$, π, and $\frac{3}{2}\pi$. From these values the analyzing powers $D_2(\theta)$, $D_{33}(\theta)$, and $[D_{11}(\theta)-D_{22}(\theta)]$ were calculated by means of Eq. (5). Theoretical curves were then fitted to these analyzing powers by means of the

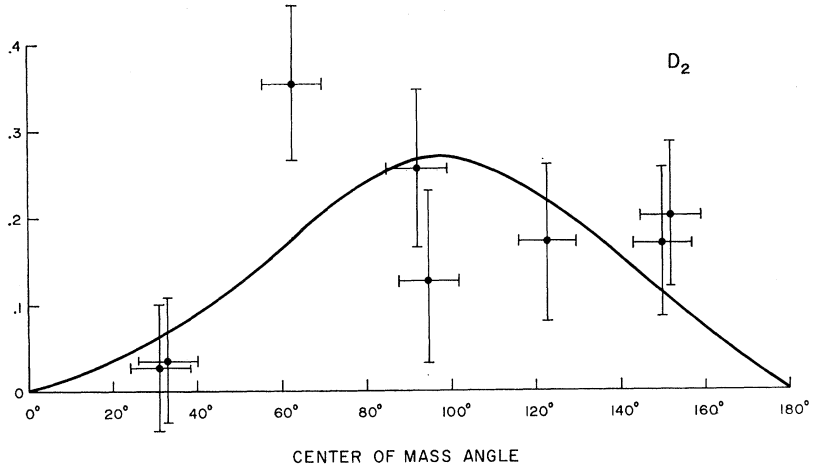

FIG. 7. Final results for the vector analyzing power $D_2(\theta)$ of the $H^2(d, p)H^3$ reaction. The curve is a least-squares fit to the data points.

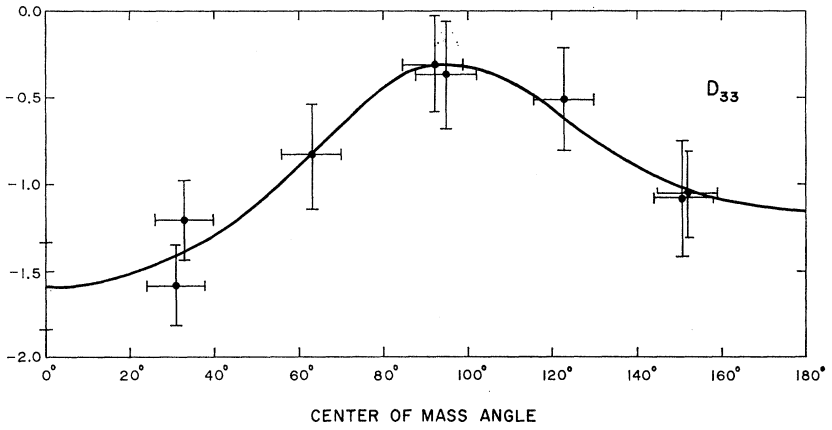

FIG. 8. Final results for the tensor analyzing power $D_{33}(\theta)$ of the $H^2(d, p)H^3$ reaction. The curve is a least-squares fit to the data points. The error bars drawn at 0° are discussed in Sec. V B.

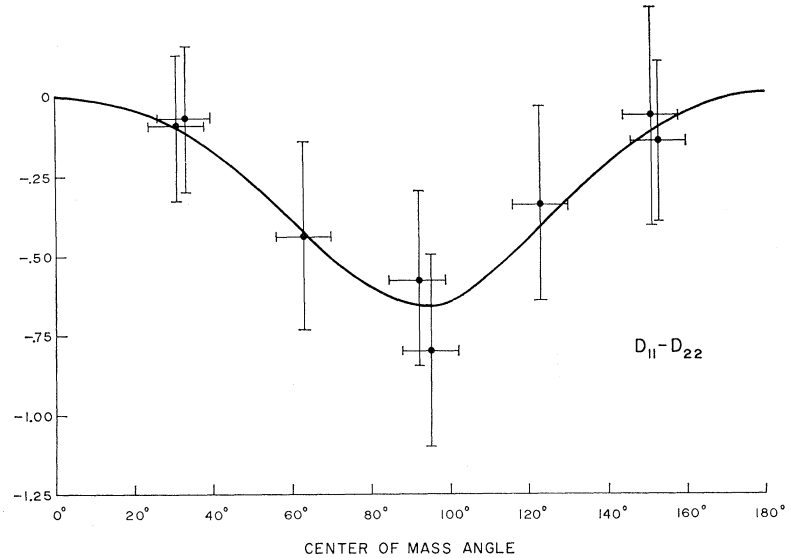

FIG. 9. Final results for the tensor analyzing power $[D_{11}(\theta) - D_{22}(\theta)]$ of the $H^2(d, p)H^3$ reaction. The curve is a least-squares fit to the data points.

expansions

$$D_2(\theta)=[W_0(\theta)]^{-1}\sum_{l=1}^{2}a_lP_{l1}(\cos\theta),$$

$$D_{33}(\theta)=[W_0(\theta)]^{-1}\sum_{l=0}^{2}b_lP_l(\cos\theta), \quad (10)$$

and

$$D_{11}(\theta)-D_{22}(\theta)=[W_0(\theta)]^{-1}\sum_{l=2}^{3}c_lP_{l2}(\cos\theta),$$

where $W_0(\theta)$, the unpolarized angular distribution, is given by[24]

$$W_0(\theta)=1+0.385P_2(\cos\theta)+0.018P_4(\cos\theta). \quad (11)$$

A matrix-inversion routine based on the method described in Ref. 25 was used for the computation of the least-squares coefficients and their standard deviations.

B. Final Experimental Values

The final experimental values obtained for $D_2(\theta)$, $D_{33}(\theta)$, and $D_{11}(\theta)-D_{22}(\theta)$ are presented in Table II, the least-squares coefficients obtained for these analyzing powers are given in Table III, while the experimental points and least-squares curves are shown in Figs. 7–9. In all cases, the errors represent statistical errors only; however, the only known source of systematic error which is likely to be as important as the statistical errors lies in the determination of the beam tensor and vector polarization. Assumptions used in the determination of the vector polarization have been discussed in Sec. IV of this paper. Any error in this determination would multiply the present results for $D_2(\theta)$ by a constant factor.

Measurement of the tensor polarization depends on knowledge of the analyzing power of the $H^3(d,n)He^4$ reaction. The analyzing power of this reaction has traditionally been calculated on the assumption that the only contributing compound nucleus was the $J^\pi=\frac{3}{2}^+$ state. However, the work of McIntyre and Haeberli[26] on the $He^3(d,p)He^4$ reaction suggests that a 5–10% contribution from the $J^\pi=\frac{1}{2}^+$ state is present in that reaction, and therefore, presumably, in the $H^3(d,n)He^4$ reaction as well. If this estimate turns out to be correct, it then follows that the polarization of the beam was 5–10% higher than measured, and, therefore, that the $H^2(d,p)H^3$ analyzing powers are lower than measured by the same amount.

The error bars shown at 0° in Fig. 8 represent an angle-independent error resulting from determination of the factor R in Eq. (9). The effect of this error is to subject the curve for $D_{33}(\theta)$ to the vertical position uncertainty whose magnitude is represented by these error bars.

TABLE IV. Comparison of experimental results on the $H^2(d,p)H^3$ vector analyzing power $D_2(\theta)$.

	Mean energy (keV)	B_3/B_0	B_4/B_0
Present data	140	0.321±0.059	−0.036±0.042
Ref. 8	100[a]	0.199±0.010	−0.046±0.011[b]
Ref. 8	200[a]	0.247±0.005	−0.075±0.008[b]
Ref. 8	300[a]	0.245±0.003	−0.084±0.003[b]
Ref. 8	400[a]	0.256±0.002	−0.086±0.008[b]
Ref. 8	500[a]	0.266±0.007	−0.095±0.007[b]
Ref. 7	460	0.297±0.009	−0.101±0.006
Ref. 6	400	0.354[c]	

[a] It is not explicitly stated in Ref. 8 whether these are incident or mean energies. We have assumed the latter.
[b] The data listed in Ref. 8 should be multiplied by −4/9. This factor has already been applied here.
[c] No error figure given in this reference.

C. Discussion

1. Comparison with Theory

Comparison of the coefficients a_l, b_l, and c_l given in Eq. (10), with the expressions shown in Eq. (6), yields the following relationships:

$$\begin{aligned} a_1&=\tfrac{2}{3}B_3/B_0,\\ a_2&=\tfrac{2}{3}B_4/B_0,\\ b_0&=2B_7/B_0,\\ b_1&=2B_8/B_0,\\ b_2&=2B_5'/B_0,\\ c_2&=3B_5/B_0,\\ c_3&=3B_{11}/B_0. \end{aligned} \quad (12)$$

Examination of Table III shows that c_3 vanishes, at least within the errors of the measurement. However, the nonvanishing of b_1 is evidence that quintet-state matrix elements are nonzero. Coefficients of higher-order Legendre functions could not be detected in the present experiment because of insufficient statistics.

2. Comparison with Other Experiments

A summary of the present experimental results on the $H^2(d,p)H^3$ analyzing powers is presented in Tables IV–VI. The data that can most directly be compared with those of the present experiment are the two sets of measurements by Ad'yasevich *et al.*[8,9] It will be noted that experimental values for the $H^2(d,p)H^3$ total cross section were needed in order to make the comparison. These data were taken from Ref. 27.

For the various coefficients, the disagreement between the present results and those of Ad'yasevich *et al.* (as

[24] R. B. Theus, W. I. McGarry, and L. A. Beach, Nucl. Phys. 80, 273 (1966); L. A. Beach (erratum by private communication).
[25] J. Orear, University of California, Lawrence Radiation Laboratory Report No. UCRL-8417, 1958, Sec. 16 (unpublished).
[26] L. C. McIntyre and W. Haeberli, Nucl. Phys. A91, 369 (1967).
[27] W. A. Wenzel and W. Whaling, Phys. Rev. 88, 1149 (1952), Table I.

TABLE V. Comparison of experimental results on the $H^2(d, p)H^3$ tensor analyzing power $D_{33}(\theta)$.

	Mean energy (keV)	B_7/B_0	B_8/B_0	B_5'/B_0
Present data	140	-0.413 ± 0.152	-0.148 ± 0.084	-0.556 ± 0.102
Ref. 9	165[a]	-0.083 ± 0.007	-0.106 ± 0.014	-0.304 ± 0.016
Ref. 9	290[a]	-0.142 ± 0.009	-0.134 ± 0.016	-0.294 ± 0.020
Ref. 9	470[a]	-0.156 ± 0.007	-0.176 ± 0.014	-0.324 ± 0.018
Ref. 7	460	-0.144 ± 0.003	-0.205 ± 0.007	-0.300 ± 0.009
Ref. 10	80			-0.41[b]±0.14

[a] It is not explicitly stated in Ref. 9 whether these are incident or mean energies. We have assumed the latter.

[b] The value listed in Ref. 10 should be multiplied by -1. This factor has already been applied here.

interpolated to the appropriate energy) generally amounts to approximately two to three times the quoted errors of the present measurements. The disagreement is taken to be a measure of the systematic errors present in these two sets of measurements. However, in view of the recent results of Fick and Franz[11] (to be discussed below), it seems possible that the 25-keV difference between the mean-deuteron energy of the Ad'yasevich data and that of the present data may be responsible for the discrepancies.

The results of the Erlangen group[10] for B_5'/B_0 are in excellent agreement with the present results. (The sign of this coefficient as given in the original paper is believed to be incorrect.) The results for B_5/B_0, however, are in disagreement with the present results, unless marked energy dependence of this coefficient is present in the range 80–140 keV. Such an energy dependence has, in fact, been reported recently by Fick and Franz.[11] The measurements reported in these papers indicate a rapidly varying, resonancelike behavior for all of the analyzing powers near 105 keV. This behavior is attributed[11] to a new 1^- level in He^4 at 23.9-MeV excitation energy above the He^4 ground state.

TABLE VI. Comparison of experimental results on the $H^2(d, p)H^3$ tensor analyzing power $[D_{11}(\theta)-D_{22}(\theta)]$.

	Mean energy (keV)	B_5/B_0	B_{11}/B_0
Present data	140	-0.059 ± 0.015	0.002 ± 0.009
Ref. 9	165[a]	-0.015 ± 0.002	-0.003 ± 0.001
Ref. 9	290[a]	0.001 ± 0.002	-0.003 ± 0.001
Ref. 9	470[a]	0.031 ± 0.002	-0.004 ± 0.001
Ref. 7	460	0.011 ± 0.001	-0.005 ± 0.001
Ref. 10	80	-0.01 ± 0.01	

[a] It is not explicitly stated in Ref. 9 whether these are incident or mean energies. We have assumed the latter.

Since the incident-deuteron energy for the Erlangen results (Ref. 10) shown in Tables V and VI was 100 keV, it is possible that these results are free from effects of the resonance, whereas the present data, with an incident energy of 190 keV and a 100-keV-thick target, must include some of the resonance effects. Further data taken with thin targets would be desirable in order to verify this explanation of the disagreement.

3. Summary

The present experiment on the $H^2(d, p)H^3$ reaction with a polarized beam and an unpolarized target has measured seven of the B coefficients [Eq. (7)] at a mean deuteron energy of 140 keV. The agreement with previous measurements at nearby energies is, in general, good enough to conclude that no major systematic errors are present in these measurements. The probable presence of quintet-state effects in the reaction has been detected at 140 keV, the lowest energy at which evidence for these effects has yet been found. Further exploration of the low-energy behavior of the quintet-state matrix elements would be of interest, since data on this behavior are relevant to the assumptions underlying a comparison of the $D+D$ reaction branches as a measure of the charge symmetry of nuclear forces.[24]

ACKNOWLEDGMENTS

We are grateful to Professor Vernon W. Hughes for encouraging and guiding this research. We also wish to thank Dominic C. Constantino for invaluable help in the construction of the apparatus and Donald R. Moler for assistance with the electronics.